Allelic Depletion of *grem1* Attenuates Diabetic Kidney Disease

Sarah A. Roxburgh,[1] Jayesh J. Kattla,[1] Simon P. Curran,[1] Yvonne M. O'Meara,[1,2] Carol A. Pollock,[3] Roel Goldschmeding,[4] Catherine Godson,[1] Finian Martin,[5] and Derek P. Brazil[1]

OBJECTIVE—Gremlin (*grem1*) is an antagonist of the bone morphogenetic protein family that plays a key role in limb bud development and kidney formation. There is a growing appreciation that altered *grem1* expression may regulate the homeostatic constraints on damage responses in diseases such as diabetic nephropathy.

RESEARCH DESIGN AND METHODS—Here we explored whether knockout mice heterozygous for *grem1* gene deletion ($grem1^{+/-}$) exhibit protection from the progression of diabetic kidney disease in a streptozotocin-induced model of type 1 diabetes.

RESULTS—A marked elevation in *grem1* expression was detected in the kidneys and particularly in kidney tubules of diabetic wild-type mice compared with those of littermate controls. In contrast, diabetic $grem1^{+/-}$ mice displayed a significant attenuation in *grem1* expression at 6 months of diabetes compared with that in age- and sex-matched wild-type controls. Whereas the onset and induction of diabetes were similar between $grem1^{+/-}$ and wild-type mice, several indicators of diabetes-associated kidney damage such as increased glomerular basement membrane thickening and microalbuminuria were attenuated in $grem1^{+/-}$ mice compared with those in wild-type controls. Markers of renal damage such as fibronectin and connective tissue growth factor were elevated in diabetic wild-type but not in $grem1^{+/-}$ kidneys. Levels of pSmad1/5/8 decreased in wild-type but not in $grem1^{+/-}$ diabetic kidneys, suggesting that bone morphogenetic protein signaling may be maintained in the absence of *grem1*.

CONCLUSIONS—These data identify *grem1* as a potential modifier of renal injury in the context of diabetic kidney disease.
***Diabetes* 58:1641–1650, 2009**

Diabetic nephropathy represents the most common cause of end-stage kidney disease worldwide, affecting approximately one-third of diabetic patients (1). Extracellular signaling molecules such as transforming growth factor (TGF)-β, connective tissue growth factor (CTGF), and advanced glycation end products are implicated as drivers of diabetic nephropathy (2). Intracellular signaling events including Smad3 phosphorylation, the phosphatidylinositol 3-kinase → protein kinase B/Akt pathway, and mitogen-activated protein kinase activation play a role in kidney cell damage during diabetic nephropathy (3–5). However, the precise molecular mechanisms underlying the pathogenesis of diabetic nephropathy remain incompletely understood, and thus additional research is needed to identify novel molecular targets that may be of potential therapeutic value.

grem1 is a highly conserved, 24–26 kDa secreted glycoprotein member of the cysteine knot superfamily, with the ability to heterodimerize and antagonize bone morphogenetic proteins (BMPs), in particular BMP-2, -4, and -7 (6). *grem1* regulates outgrowth, chondrogenesis, and apoptosis of the developing limb bud (6–8), as well as branching morphogenesis during kidney development (9). Mice homozygous for deletion of *grem1* die of complete renal agenesis shortly after birth, supporting a primary role for *grem1* in the developing kidney (10,11). Recent data have identified a role for *grem1* in bone formation and bone mass (12,13), as well as in pulmonary hypertension (14) and angiogenesis (15). A role for *grem1* in diabetic nephropathy was originally proposed by data from our group that identified *grem1* upregulation in primary human mesangial cells treated with high glucose and in kidneys of diabetic rats (16,17). *grem1* was also upregulated in other in vitro models relevant to diabetic nephropathy, such as mesangial cells subjected to cyclical mechanical strain or TGF-β1, and, importantly, in biopsy specimens from patients with diabetic nephropathy (18–20). We recently demonstrated that *grem1* upregulation is part of the transcriptomic response of tubular epithelial cells exposed to TGF-β1 (20). Increasing evidence suggests that the degree of *grem1* expression correlates with disease severity in a variety of forms of renal fibrosis, including glomerular scarring in in vivo acute glomerulonephritis (21), tubular scarring in chronic allograft nephropathy, and progressive membranous nephropathy (22). Levels of *grem1* in the adult kidney are low, and disease-dependent upregulation of *grem1* in diabetic nephropathy may reflect a reactivation of quiescent gene expression in response to hyperglycemia and other stimuli (23). Together, these data point toward a contributory role for *grem1* in diabetic microvascular complications.

From the [1]University College Dublin Diabetes Research Centre, School of Medicine and Medical Science, University College Dublin, Belfield, Dublin, Ireland; [2]Mater Misericordiae University Hospital, University College Dublin Conway Institute, University College Dublin, Belfield, Dublin, Ireland; the [3]Kolling Institute, University of Sydney, New South Wales, Australia; the [4]Department of Pathology, University Medical Center Utrecht, Utrecht, the Netherlands; and the [5]School of Biomolecular and Biomedical Science, University College Dublin, Belfield, Dublin, Ireland.
Corresponding author: Derek P. Brazil, derek.brazil@ucd.ie.
Received 5 October 2008 and accepted 9 April 2009.
Published ahead of print at http://diabetes.diabetesjournals.org on 28 April 2009. DOI: 10.2337/db08-1365.

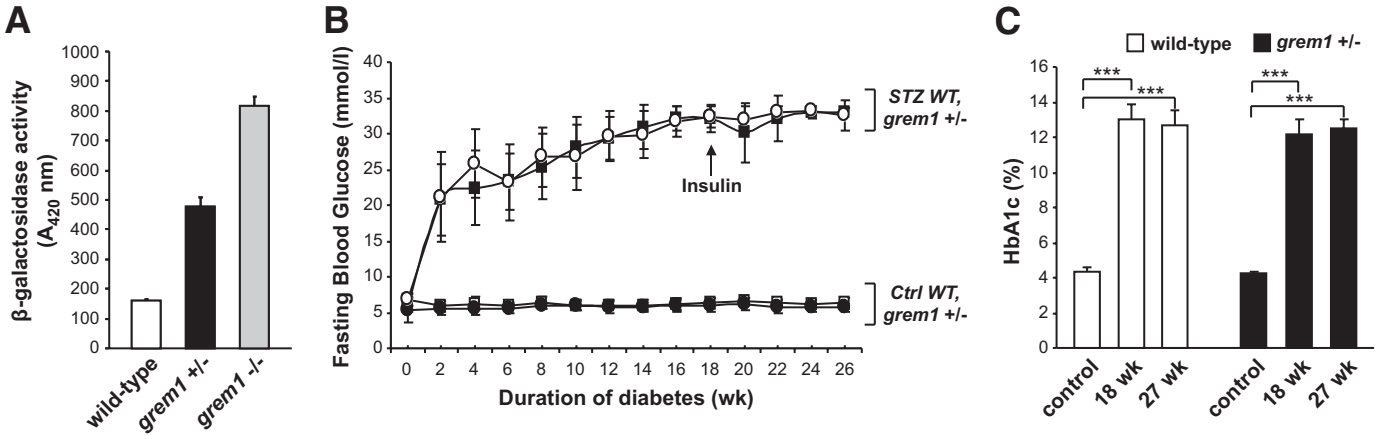

FIG. 1. Induction of type 1 diabetes in wild-type (WT) and *grem1*$^{+/-}$ mice. *A*: *grem1* promoter activity was examined in embryonic fibroblasts from embryonic day 13.5 mouse embryos. Lysates from wild-type ($^{+/+}$), *grem1*$^{+/-}$, or *grem1*$^{-/-}$ cells were assayed for β-galactosidase activity as described. Results are representative of four experiments carried out in duplicate. *B*: Wild type and *grem1*$^{+/-}$ mice were injected intraperitoneally with either citrate buffer (control [ctrl]) or 50 mg/kg STZ for 5 consecutive days (week 0) according to established procedures (RESEARCH DESIGN AND METHODS). Fasting blood glucose levels were monitored biweekly for 27 weeks using a glucometer and a drop of blood from the tail vein. Significant increases in blood glucose levels developed in both groups after 2 weeks ($P < 0.001$, $n = 10–12$ mice per group) and were maintained over the 27 weeks study time course. □, wild-type control; ●, *grem1*$^{+/-}$ control; ■, wild-type diabetic; ○, *grem1*$^{+/-}$ diabetic. *C*: Whole blood was collected via cardiac puncture at time of sacrifice in both cohorts of mice. Percent A1C was assessed via ELISA as described in RESEARCH DESIGN AND METHODS. A significant increases in percent A1C were detected in both cohorts at 18 and 27 weeks of diabetes (mean ± SE). ***$P < 0.001$, using one-way ANOVA and Tukey-Kramer multiple comparison test, $n = 6–11$ in each group.

In this study, we addressed the hypothesis that reduced *grem1* gene expression would provide protection in the diabetic kidney. Our data suggest that depletion of *grem1* expression in mice attenuates early diabetic nephropathy–like changes in kidney.

RESEARCH DESIGN AND METHODS

All animal procedures were licensed by the Irish Department of Health and Children and approved by the local animal research ethics committee at University College Dublin. *grem1* heterozygote knockout mice (*grem1*$^{+/-}$) were generated by Richard Harland, University of California at Berkeley (Berkeley, CA) (10). Experimental animals were generated by crossing wild-type C57BL/6J and *grem1*$^{+/-}$ mice, with male offspring used in the study. Mice were maintained in a conventional animal facility in standard caging, with free access to water and standard rodent chow. Genotyping was performed using DNA extracted from ear punches as described previously (10).

Induction of type 1 diabetes in mice. Seven- to 10-week-old male mice (both wild-type and *grem1*$^{+/-}$), weighing ~19 g at the onset of the experimental protocol were genotyped and then randomly divided into two groups: A, treated with streptozotocin (STZ) (Sigma) dissolved in 100 mmol/l citrate buffer, pH 4.5; or B, treated with citrate buffer alone (http://www.amdcc.org). STZ was dissolved in sterile citrate buffer and injected intraperitoneally (50 mg/kg) within 10 minutes of preparation on 5 consecutive days. Fasting blood glucose levels were assayed after a 6-h fast between 8:00 A.M. and 2:00 P.M. with tail venipuncture at 2:00 P.M. Diabetes was confirmed by two consecutive daily measurements of fasting blood glucose >15 mmol/l 2 weeks after STZ injection. To maintain weight and prevent ketoacidosis, long-acting insulin (Insulotard, Nova Nordisk) subcutaneously at a dose of ⅓ IU three times weekly was started in all diabetic mice at week 18 of diabetes.

Tissue pathology and urine collection. Mice were housed individually in mouse metabolic cages (Technoplast) for 24 h to collect urine 5 days before sacrifice. Urine volumes were recorded, and urinary glucose, ketone, and erythrocyte levels were monitored semiquantitatively with Multistix reagent strips (Bayer). Cardiac puncture was performed at the time of sacrifice. The left renal artery was clamped and the left kidney was removed, weighed, and dissected. The inferior renal pole was promptly processed for electron microscopy, and the superior renal pole was snap-frozen and stored at −80°C for RNA and protein extraction. Renal perfusion was performed via cannulation of the left ventricle with an 18-gauge needle. Initial perfusion using gravity was performed with sterile normal saline (pH 7.4) for 5 min, followed by 4% (wt/vol) paraformaldehyde (pH 7.4) for 5 min. The perfused right kidney was then removed and incubated in 4% paraformaldehyde for 24 h at room temperature. Kidneys were processed, cut at 3-μm thickness on a rotary microtome, and stained with hematoxylin/eosin, periodic acid Schiff, or picrosirius red. Stained sections were scored independently (single-blinded) by pathologists using normal light microscopy. The amount of mesangial matrix was scored with periodic acid Schiff staining (score 1–4). Collagen distribution in the cortex was scored with Sirius red staining using a normal light microscope (score 1–5).

Clinical biochemistry. Urinary albumin was measured using an Albuwell M kit, and urinary creatinine was measured using a Creatinine Companion murine ELISA kit (Exocell, Philadelphia, PA). Urine was collected in metabolic cages, urine volume was recorded, and 24-h urinary albumin excretion levels were assayed with the Albuwell M assay kit.

Plasma creatinine, serum lipids, and whole blood A1C were measured at the Mouse Metabolic Phenotyping Core, Vanderbilt Medical Center (Nashville, TN). Plasma creatinine was measured on a high-performance liquid chromatography Zorbax SCX strong cation exchange column (Agilent, Wilmington, DE) as described previously (http://www.amdcc.org). A1C was measured using a DCA 2000 analyzer and cartridges (Bayer). Total plasma cholesterol and triglycerides were measured by standard enzymatic assays (Raichem). HDL cholesterol was measured after precipitation of VLDL and LDL using dextran sulfate and magnesium.

Estimation of creatinine clearance. Creatinine clearance was calculated using the equation (urine volume [microliters] × urine creatinine [milligrams per deciliter])/(serum creatinine [milligrams per deciliter] × 1,440 [minutes]) and then corrected to total body weight at sacrifice (grams) to give creatinine clearance in microliters per minute per gram body weight.

Electron microscopy. The left inferior kidney pole was removed, diced into 1-mm cubes, and fixed in 2.5% (v/v) glutaraldehyde in 0.1 mol/l cacodylate buffer. The samples were washed in 0.1 mol/l cacodylate buffer and then postfixed in 1% (wt/vol) aqueous osmium tetroxide. The tissues were washed, dehydrated through a graded series of ethanols, and embedded in Spurr resin. Thick sections (0.5 μm) were cut, affixed to glass slides, stained with toluidine blue, and viewed by light microscopy. Thin (100 nm) sections were cut from selected areas and viewed with an FEI CM-12 transmission electron microscope operated at 80 keV. Glomerular basement membrane (GBM) thickness measurements were assessed as follows: two to four glomeruli were randomly selected in each slide, and serial measurements were taken at intervals from the margins of the lamina rara interna to lamina rara externa. Images were taken and analyzed with an AMT XR41 digital TEM camera system. Up to 60 measurements were taken per kidney.

Quantitative PCR. Total RNA was isolated from snap-frozen renal poles by homogenization in 1 ml TRIzol (GibcoBRL, Life Technologies) using a Polytron (Kinematica) and a Qiagen RNeasy kit. Reverse transcription was performed using SuperScript II (Invitrogen), followed by quantitative real-time PCR on an ABI Prism 7700 sequence detection system. Mouse *grem1* (Mm00488615 S1), BMP-7 (Mm00432102 m1), fibronectin (Mm00482221), vimentin (Mm00432102 m1), and CTGF (Mm00515790 g1) real-time oligo probes were purchased from Applied Biosystems.

Western Blotting. Portions of the renal pole were lysed in radioimmunoprecipitation assay buffer containing 50 mmol/l Tris-HCl (pH 7.4), 1% (vol/vol)

TABLE 1
Metabolic and renal function parameters of control and diabetic mice

Group/parameter	Control (+/+)	Diabetic (+/+)		Control *grem1*$^{+/-}$	Diabetic *grem1*$^{+/-}$	
		18 weeks	27 weeks		18 weeks	27 weeks
Body weight						
Initial (g)	19.37 ± 0.61 (10)	22.3 ± 1.17 (6)	19.3 ± 0.85 (10)	20.15 ± 0.71 (11)	23.91 ± 1.43 (6)	20.02 ± 0.47 (12)
Final (g)	32.00 ± 1.41 (10)	20.64 ± 1.24 (6)‡	22.82 ± 1.15 (10)*	30.95 ± 0.66 (11)	21.84 ± 1.29 (6)*	22.49 ± 0.84 (12)*
Fasting plasma glucose						
Initial (mmol/l)	6.06 ± 0.38 (8)	6.32 ± 0.18 (6)	6.05 ± 0.34 (10)	5.4 ± 0.27 (11)	5.68 ± 0.23 (6)	6.79 ± 0.27 (12)
Final (mmol/l)	6.28 ± 0.17 (10)	>33.3 ± 0 (6)*	33.02 ± 0.19 (10)*	5.73 ± 0.21 (11)	>33.3 ± 0 (6)*	32.64 ± 0.65 (12)*
A1C (%)	4.35 ± 0.26 (6)	13.06 ± 0.79 (5)*	12.65 ± 0.84 (6)*	4.26 ± 0.08 (9)	12.17 ± 0.84 (7)*	12.51 ± 0.53 (11)*
Urine volume before sacrifice (ml)	3.35 ± 0.93 (9)	15.32 ± 4.58 (6)†	15.18 ± 2.96 (10)‡	4.32 ± 0.87 (13)	18.59 ± 5.95 (6)‡	12.31 ± 3.19 (11)†
Left kidney weight (g)	0.168 ± 0.01 (10)	0.185 ± 0.01 (6)	0.204 ± 0.01 (10)‡	0.167 ± 0.01 (11)	0.202 ± 0.01 (6)†	0.199 ± 0.01 (11)†
Left kidney–to–total body weight ratio (g/kg)	5.409 ± 0.19 (10)	9.074 ± 0.27 (6)*	9.077 ± 0.38 (10)*	5.536 ± 0.16 (11)	9.152 ± 0.63 (6)*	8.816 ± 0.28 (11)*
Plasma creatinine (mg/dl)	0.072 ± 0.01 (12)	0.043 ± 0.01 (6)†	0.042 ± 0.01 (8)‡	0.085 ± 0.01 (11)	0.093 ± 0.01 (6)	0.071 ± 0.01 (9)
Creatinine clearance (μl · min^{-1} · g body wt^{-1})	13.72 ± 1.35 (8)	35.39 ± 7.14 (8)†	27.45 ± 3.89 (8)	9.07 ± 0.71 (10)	16.87 ± 3.44 (5)	35.11 ± 6.37 (8)*
ACR	63.51 ± 15.25 (9)	636.5 ± 341.4 (3)	594.96 ± 664.04 (6)†	104.13 ± 13.7 (11)	284.76 ± 52.49 (3)	287.1 ± 68.75 (8)
Urinary albumin excretion rate (24 h)	34.02 ± 4.54 (9)	129.59 ± 27.51 (6)‡	129.32 ± 16.05 (8)*	33.09 ± 3.003 (11)	101.23 ± 26.17 (3)	85.71 ± 20.82 (8)†
Total cholesterol (g/dl)	142.12 ± 8.36 (8)	129.67 ± 34.60 (3)	114.1 ± 6.26 (8)†	123.3 ± 10.51 (10)	170.0 ± 9.60 (5)‡	113.14 ± 9.24 (7)
HDL cholesterol (g/dl)	77 ± 3.69 (8)	62.73 ± 3.52 (6)†	59.4 ± 4.19 (10)‡	58.3 ± 2.90 (9)	60 ± 4.48 (6)	51.29 ± 4.93 (7)
Triglycerides (g/dl)	102 ± 13.10 (8)	172.55 ± 27.7 (6)†	158.2 ± 21.38 (10)†	78 ± 6.11 (10)	124.5 ± 16.73 (6)†	130.71 ± 10.71 (7)‡
LDL cholesterol (g/dl)	34.43 ± 3.07 (7)	47.25 ± 17.00 (4)	31.87 ± 5.89 (8)	41.87 ± 6.79 (8)	85.5 ± 13.86 (4)‡	33.43 ± 6.80 (7)

Data are expressed as means ± SE (number of animals per group). Data were compared using one-way ANOVA and Tukey-Kramer post hoc analysis. *$P < 0.001$; †$P < 0.05$; ‡$P < 0.01$; compared with age-matched controls of the same genetic type.

Nonidet P-40, 0.25% (vol/vol) sodium deoxycholate, 150 mmol/l NaCl, and 1 mmol/l EDTA, supplemented with fresh 1 mmol/l phenylmethylsulfonyl fluoride, 1× protease inhibitor cocktail (Sigma), 1 mmol/l NaF, 40 mmol/l β-glycerophosphate, 2 μmol/l Microcystin, and 1 mmol/l sodium vanadate. Protein extracts (25 μg) were then separated by 10% (vol/vol) SDS-PAGE and blotted using phospho-Smad1/5/8 (95115; Cell Signaling), total Smad1/5/8 (sc-6031R; Santa Cruz), BMP-7 (ab27569; Abcam), or β-actin (Sigma) antibodies exactly as described previously (4).

Statistical analysis. All data were plotted as mean ± SE. Student's two-tailed *t* tests or one-way ANOVA with Tukey-Kramer multiple comparison post hoc tests were calculated using the Instat software package.

RESULTS

Induction of type 1 diabetes in wild-type and *grem1*$^{+/-}$ mice. Using the replacement β-galactosidase "knock-in" gene activity as a marker of *grem1* promoter activity (10), *grem1* gene expression was detected in heterozygous *grem1*$^{+/-}$ knockout cells (Fig. 1*A*). Homozygous *grem1*$^{-/-}$ knockout mouse embryonic fibroblasts displayed approximately double the activity of β-galactosidase, suggesting that maximal *grem1* expression required both copies of the *grem1* gene. We therefore hypothesized that *grem1* expression would be reduced in the kidneys of *grem1*$^{+/-}$ mice in response to hyperglycemia.

Type 1 diabetes was induced in *grem1*$^{+/-}$ and wild-type mice using STZ, with time zero defined as the day of initial STZ injection. Mice were maintained in the diabetic state for 18 or 27 weeks. Metabolic parameters, body weight, renal weight, and serum glucose levels are presented in Table 1. Nondiabetic mice gained significant weight compared with diabetic mice, as assessed at study end (wild-type control mice body weight 32.0 ± 4.47 g; wild-type diabetic mice body weight 22.82 ± 3.22 g). No significant difference in total body weight between wild-type and *grem1*$^{+/-}$ mice in either the control or diabetic cohorts was detected (Table 1). Both diabetic groups developed marked fasting hyperglycemia that peaked at ~33 mmol/l and was maintained up to the 27-week time point (Fig. 1*B*). The onset and severity of hyperglycemia were similar between wild-type and *grem1*$^{+/-}$ mice (Fig. 1*B*). Marked and significant increases in A1C levels in diabetic mice were also detected at 18 and 27 weeks of hyperglycemia (Fig. 1*C*), in both wild-type and *grem1*$^{+/-}$ groups. Thus, the onset, severity, and progression of diabetes were similar in both wild-type and *grem1*$^{+/-}$ mice.

***grem1* upregulation is reduced in *grem1*$^{+/-}$ mice kidneys.** We assessed the effects of type 1 diabetes on *grem1* expression in kidneys from our experimental animals. Minimal *grem1* mRNA was detected in wild-type and *grem1*$^{+/-}$ control kidneys at both time points examined but the amount was dramatically increased in wild-type diabetic mice (Fig. 2*A*). Approximately 62-fold increased *grem1* upregulation was detected at 18 weeks compared with 42-fold at 27 weeks in wild-type diabetic mice (Fig. 2*B*). In contrast, *grem1*$^{+/-}$ mice manifested a 53-fold increase at 18 weeks and an 8-fold increase at 27 weeks in diabetic kidney (Fig. 2*B*). The fold change in *grem1* mRNA upregulation at 27 weeks in diabetic *grem1*$^{+/-}$ mice was significantly lower than that seen in diabetic wild-type mice at the same time point (Fig. 2*B*). Increased *grem1* protein was also detected in diabetic wild-type kidney sections compared with that in controls via Western blotting and immunohistochemistry (Fig. 2*C* and *D* and supplementary Fig. 1, available in an online appendix at http://diabetes.diabetesjournals.org/cgi/content/full/db08-1365/DC1). In contrast, the increase in *grem1* protein was blunted in diabetic *grem1*$^{+/-}$ mice (Fig. 2*C* and *D*). These

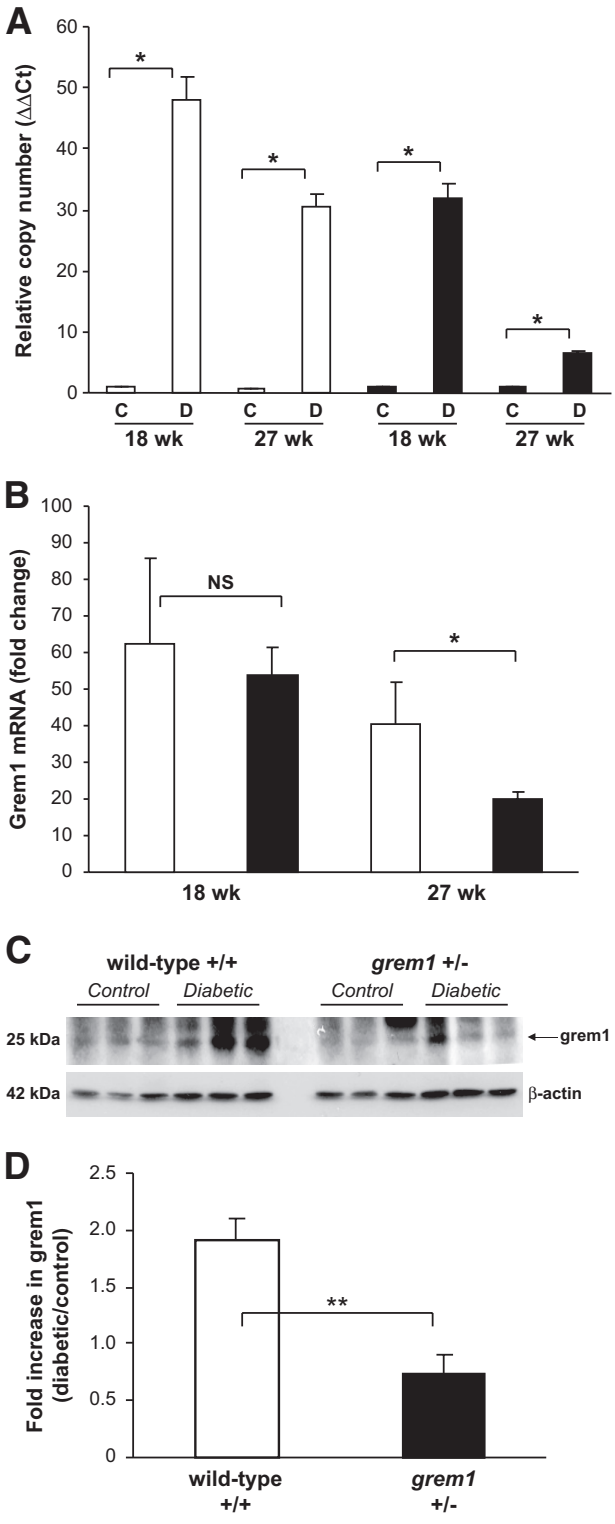

FIG. 2. Diabetes-mediated induction of *grem1* expression is attenuated in *grem1*$^{+/-}$ mice. *A*: Total RNA was extracted from renal poles of control (C) and diabetic (D) wild-type (□) and *grem1*$^{+/-}$ (●) mice at each time point indicated. A quantitative TaqMan PCR was performed using mouse *grem1* specific oligonucleotides as described. ΔΔCt values were calculated by subtracting the Ct values for the *18S* control from the corresponding *grem1* value obtained in the same tube, and altered mRNA levels were then calculated by setting the control in each age-group to 1. Data are plotted as mean ± SE. *$P < 0.05$, Student's unpaired *t* test, $n = 4–6$ for each group. *B*. Fold change in *grem1* mRNA was calculated by dividing the ΔΔCt value for diabetic mice by the mean of the corresponding age-matched control group. Data are plotted as mean fold change ± SE. *$P < 0.05$, Student's unpaired *t* test, $n = 4–6$ per group. *C*: Protein extracts (20 μg) from control and diabetic wild-type and *grem1*$^{+/-}$ renal poles were probed by Western blot with *grem1* antibody (R&D Systems) and β-actin (Sigma). An approximately 25-kDa band corresponding to *grem1* was detected. *D*: Densitometry was performed using Scion Image software, and the intensity of *grem1* expression was normalized to the β-actin loading control. Data were then plotted as diabetic/control fold change for both wild-type and *grem1*$^{+/-}$ mice. **$P < 0.01$, Student's *t* test, $n = 3$.

data suggest that deletion of one copy of the *grem1* gene dramatically reduced *grem1* induction in the diabetic mouse kidney.

Early type 1 diabetes–induced structural changes are attenuated in *grem1*$^{+/-}$ kidney compared with those in wild-type kidney. Diabetic mice developed marked polyuria compared with that in age-matched controls, with no significant difference between wild-type and *grem1*$^{+/-}$ cohorts observed at 27 weeks (wild-type control urine volume 3.35 ± 2.79 ml, wild-type diabetic urine volume 15.18 ± 9.35 ml, $P < 0.01$; *grem1*$^{+/-}$ control urine volume 4.32 ± 3.15 ml, *grem1*$^{+/-}$ diabetic urine volume 12.31 ± 10.6, $P < 0.05$) (Table 1). A significant increase in the ratio of left kidney weight–to–total body weight occurred in all diabetic animals compared with that in age-matched control animals after 27 weeks of diabetes, suggestive of renal hypertrophy (wild-type control vs. diabetic 5.409 ± 0.19 vs. 9.077 ± 0.38, $P < 0.001$; *grem1*$^{+/-}$ control vs. diabetic 5.536 ± 0.16 vs. 8.816 ± 0.28, $P < 0.001$) (Table 1). The fold change in left kidney weight–to–total body weight was not significantly different between wild-type and *grem1*$^{+/-}$ mice (data not shown).

All diabetic mice developed a significant increase in GBM thickness compared with that in nondiabetic age-matched controls at 27 weeks of hyperglycemia (Fig. 3*A* and *B*). Interestingly, this increase was significantly greater in diabetic wild-type compared with that in diabetic *grem1*$^{+/-}$ mice. GBM thickness increased 47% from baseline mean in age-matched control versus diabetic wild-type mice (Fig. 3*B*, □). In contrast, a more modest 14% increase in GBM thickening was detected in control versus diabetic *grem1*$^{+/-}$ mice at 27 weeks (Fig. 3*B*, ■). The fold change in GBM thickening was significantly lower in *grem1*$^{+/-}$ mice compared with that in wild-type mice (Fig. 3*C*), suggesting that allelic depletion of *grem1* prevented diabetes-induced early structural changes in the kidney.

Moderate increases in glomerular matrix secretion and interstitial collagen deposition were observed in diabetic wild-type and *grem1*$^{+/-}$ mice compared with those in controls (Fig. 4*A* and *C*). No significant tubulointerstitial fibrosis was detected in either genotype up to 27 weeks of diabetes (data not shown). Scoring of these sections revealed that the degree of increased staining of these markers of renal damage was not significantly different between diabetic wild-type and *grem1*$^{+/-}$ mice (Fig. 4*B* and *D*). These data suggest that our model of type 1 diabetes in mice on a C57BL/6J background manifest early diabetic nephropathy–like changes in kidney but do not develop more advanced renal disease.

Diabetic *grem1*$^{+/-}$ mice exhibit attenuated changes in albumin-to-creatinine ratio and estimated glomerular filtration rate. Urinary microalbumin was increased in diabetic wild-type mice compared with that in controls (control 34.02 ± 4.53 μg, diabetic 27 weeks 129.32 ± 16.05 μg, $P < 0.001$) (Fig. 5*A*). In contrast, microalbuminuria was less severe in diabetic *grem1*$^{+/-}$ mice (control 33.09 ± 3.00 μg, diabetic 27 weeks 71.47 ± 17.54 μg, $P <$

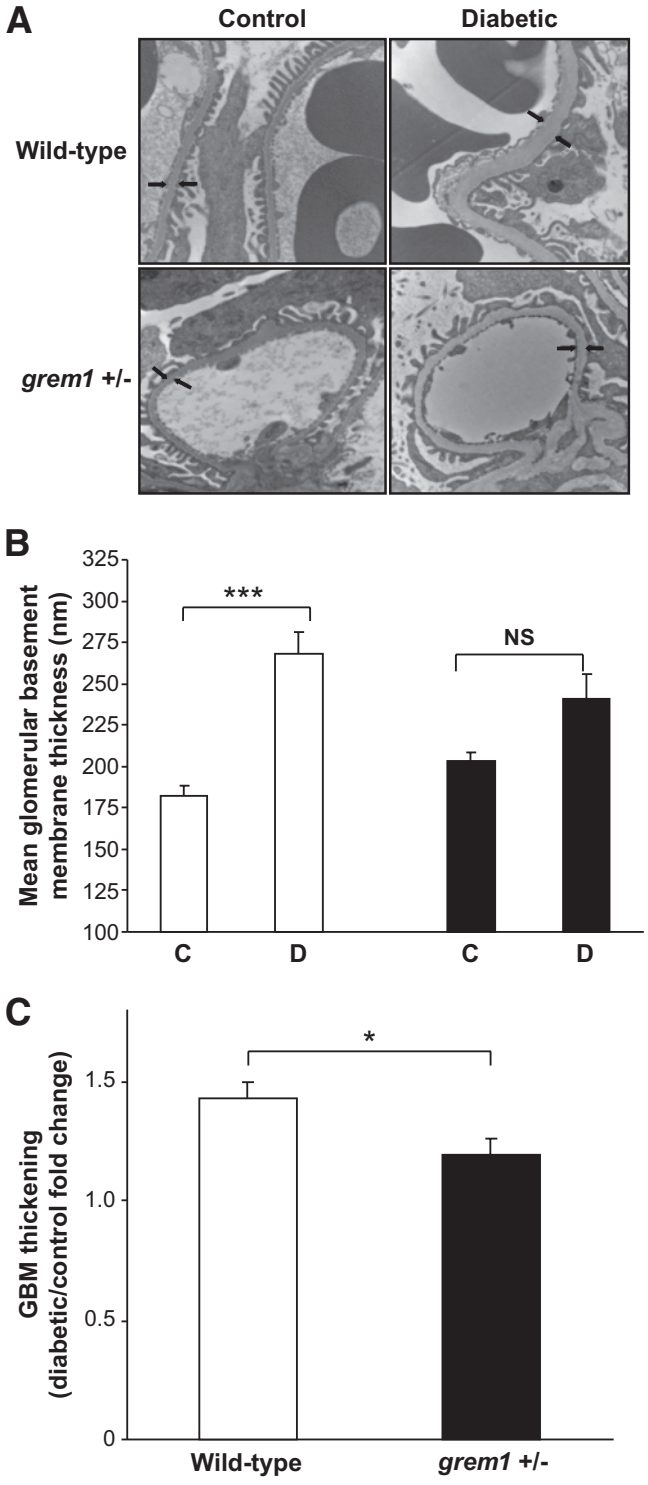

FIG. 3. Glomerular basement membrane thickening is attenuated in diabetic *grem1*$^{+/-}$ mice compared with wild-type. Kidney pieces were processed as described in RESEARCH DESIGN AND METHODS, and 100-nm sections were cut from the renal pole harvested from control and diabetic wild-type and *grem1* ± mice at 27 weeks. Sections were viewed with an FEI CM-12 transmission electron microscope operated at 80 keV. Glomeruli were randomly selected, viewed at ×15,000 magnification and serial measurements along the GBM were assessed. Arrows indicate the position of the glomerular basement membrane (*A*). Top left, nondiabetic wild-type ($^{+/+}$) control; top right, diabetic wild-type ($^{+/+}$); bottom left, nondiabetic *grem1*$^{+/-}$ control; bottom right, diabetic *grem1*$^{+/-}$. Arrows indicate the thickness of the GBM. *B* and *C*: Quantitation of GBM thickness from all groups of mice. Up to 60 serial measurements were made from each individual glomerulus, and a mean value per mouse was calculated. Data are plotted as group means ± SE. GBM thickness was significantly higher in wild-type diabetic mice compared with nondiabetic controls ($P < 0.001$ using one-way ANOVA and Tukey-Kramer multiple comparison test, $n = 7$–11 per group). The increase observed in diabetic *grem1*$^{+/-}$ mice compared with controls did not reach significance ($P = 0.224$). Fold change in GBM thickening. Mean GBM thickness values for each diabetic animal were divided by the mean thickness for control mice for both wild-type and *grem1*$^{+/-}$ groups. Mean fold change values were calculated for both wild-type and *grem1*$^{+/-}$ mice at 27 weeks. *$P < 0.05$, Student's two-tailed *t* test. □, wild type; ■, *grem1*$^{+/-}$.

0.05) (Fig. 5*A*). Fold change in microalbuminuria was significantly lower in *grem1*$^{+/-}$ diabetic mice compared with that in wild-type mice at 27 weeks of diabetes (Fig. 5*B*). These data suggest that depletion of *grem1* expression reduced the microalbuminuria associated with early renal damage in diabetic nephropathy. Serum creatinine levels decreased significantly in wild-type diabetic mice compared with those in age-matched controls (Table 1). This decrease in serum creatinine did not occur in *grem1*$^{+/-}$ mice at either 18 or 27 weeks of diabetes (Table 1). Albumin-to-creatinine ratios (ACRs) increased in diabetic wild-type mice at both 18 and 27 weeks of hyperglycemia (control 63.51 ± 15.25 μg/mg, diabetic 27 weeks 594.97 ± 271.09 μg/mg) (Fig. 5*C*). This increased ACR was greatly attenuated in diabetic *grem1*$^{+/-}$ mice (control 104.13 ± 13.68 μg/mg, diabetic 27 weeks 287.10 ± 68.75 μg/mg) (Fig. 5*C*). The smaller increase in *grem1*$^{+/-}$ mice was highlighted when fold change was calculated, showing a significantly lower increase in the ACR in *grem1*$^{+/-}$ mice compared with that in wild-type mice at 27 weeks (Fig. 5*D*).

Creatinine clearance increased in diabetic wild-type mice compared with that in controls at 18 weeks of diabetes, suggesting that glomerular hyperfiltration was occurring at this time point (Fig. 5*E*). In contrast, diabetic *grem1*$^{+/-}$ mice did not develop significant increases in creatinine clearance until the 27-week time point (Fig. 5*E*). A significantly higher fold change in creatinine clearance was detected in *grem1*$^{+/-}$ mice compared with that in wild-type mice at 27 weeks, suggesting that *grem1* depletion delayed the onset of peak hyperfiltration in diabetic mice (Fig. 5*F*).

Serum lipids were elevated in diabetic wild-type mice, showing a significant increase in triglycerides and decrease in HDL typical of diabetic hyperlipidemia (Table 1). Diabetic *grem1*$^{+/-}$ mice also manifested a significant elevation in serum triglycerides but demonstrated a significantly lower HDL at baseline than wild-type controls, in which HDL failed to drop significantly in the setting of diabetes (wild-type control 77 ± 3.69 g/dl, *grem1*$^{+/-}$ control 58.3 ± 2.9 g/dl) (Table 1).

***grem1* mRNA correlates with early indexes of diabetic nephropathy.** A significant correlation was detected between ACR and GBM thickening in both control and diabetic mice in our study (Fig. 6*A*). To assess whether *grem1* mRNA correlated with indexes of early diabetic kidney disease, *grem1* levels were compared with changes in microalbuminuria and GBM thickening. The degree of *grem1* expression correlated significantly with both ACR and GBM thickening in wild-type control and diabetic mice across the entire experiment (Fig. 6*B* and *C*). These data suggested that increased *grem1* gene expression occurred in parallel with cellular damage during early diabetic kidney disease.

To explore the mechanism of partial protection from diabetes-induced damage in *grem1*$^{+/-}$ mice, we measured

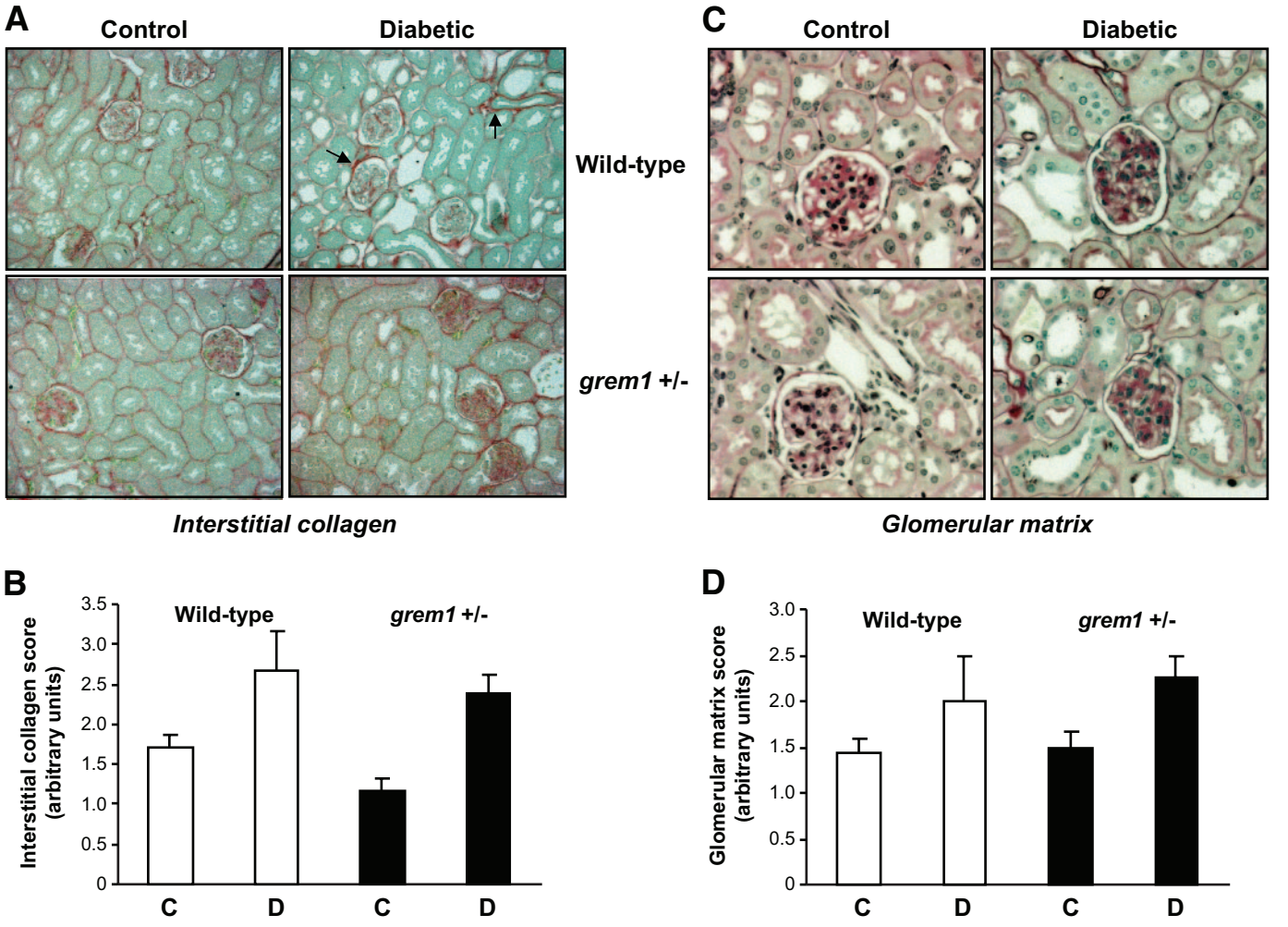

FIG. 4. Mild structural changes are evident in diabetic wild-type and *grem1*$^{+/-}$ mice by light microscopy. Post mortem, mouse kidneys were fixed by perfusion fixation in situ using 4% (wt/vol) paraformaldehyde, and 3-μm paraffin-embedded sections were stained with (*A*) Picrosirius red to detect interstitial collagen or (*C*) periodic acid Schiff to assess glomerular matrix secretion. Slides ($n = 5$ for each group) were scored blindly by an independent renal pathologist on a scale of 0–4. Data are plotted as mean scores ± SE for control (C) or diabetic (D) mice in wild-type (□) or *grem1*$^{+/-}$ (■) mice. Observed increases in both glomerular matrix secretion (*B*) or collagen staining (*D*) did not reach significance using Student's two-tailed *t* test. (A high-quality digital representation of this figure is available in the online issue.)

levels of genes implicated in kidney damage during diabetic nephropathy. Increased levels of fibronectin, vimentin, and CTGF were detected in diabetic wild-type kidney at 27 weeks (Fig. 7). In contrast, no significant increase was detected in *grem1*$^{+/-}$ diabetic kidney, suggesting that decreased *grem1* levels reduce diabetes-mediated upregulation of genes involved in mediating glomerular and renal damage. Because *grem1* is a negative regulator of BMP-7, a molecule that has been shown to mediate repair processes in the damaged kidney, we examined the effect of *grem1* deletion on this protein. No significant changes in BMP-7 mRNA or protein levels were detected at either 18 or 27 weeks of diabetes in either wild-type or *grem1*$^{+/-}$ mice (supplementary Fig. 2, available in an online appendix, and data not shown). Similar to previous reports (24), levels of phospho-Smad1/5/8, a downstream target of BMP-7 signaling, were reduced in wild-type diabetic kidney at 27 weeks (Fig. 8*C* and *D*). In contrast, no significant decrease in pSmad1/5/8 levels was detected in *grem1*$^{+/-}$ mice, possible suggesting that BMP signaling is maintained in the diabetic kidney when levels of *grem1* are reduced.

DISCUSSION

The BMP antagonist, *grem1*, regulates critical processes controlling limb-bud outgrowth and kidney development (6–8,10,11). Increased *grem1* levels correlated with the pathogenesis of diabetic nephropathy and/or progressive renal fibrosis (19,20). To address whether *grem1* depletion would protect against diabetes-induced renal disease, we evaluated renal damage in type 1 diabetic mice lacking one copy of the *grem1* gene (*grem1*$^{+/-}$). We provide the first evidence that allelic depletion of *grem1* causes a reduction in *grem1* expression levels and protects against early diabetic nephropathy–like changes in the kidney.

grem1$^{+/-}$ mice on a C57BL/6J background were used in this study. Previous data compared the susceptibility of different genetic strains of mice and showed that C57BL/6J mice were "high responders" in terms of STZ-induced hyperglycemia (25). Consistent with these findings, severe and sustained hyperglycemia developed in both wild-type and *grem1*$^{+/-}$ mice (Fig. 1*B*). We demonstrate here that type 1 diabetes induced *grem1* kidney mRNA and protein in wild-type mice. This reactivation of *grem1* expression

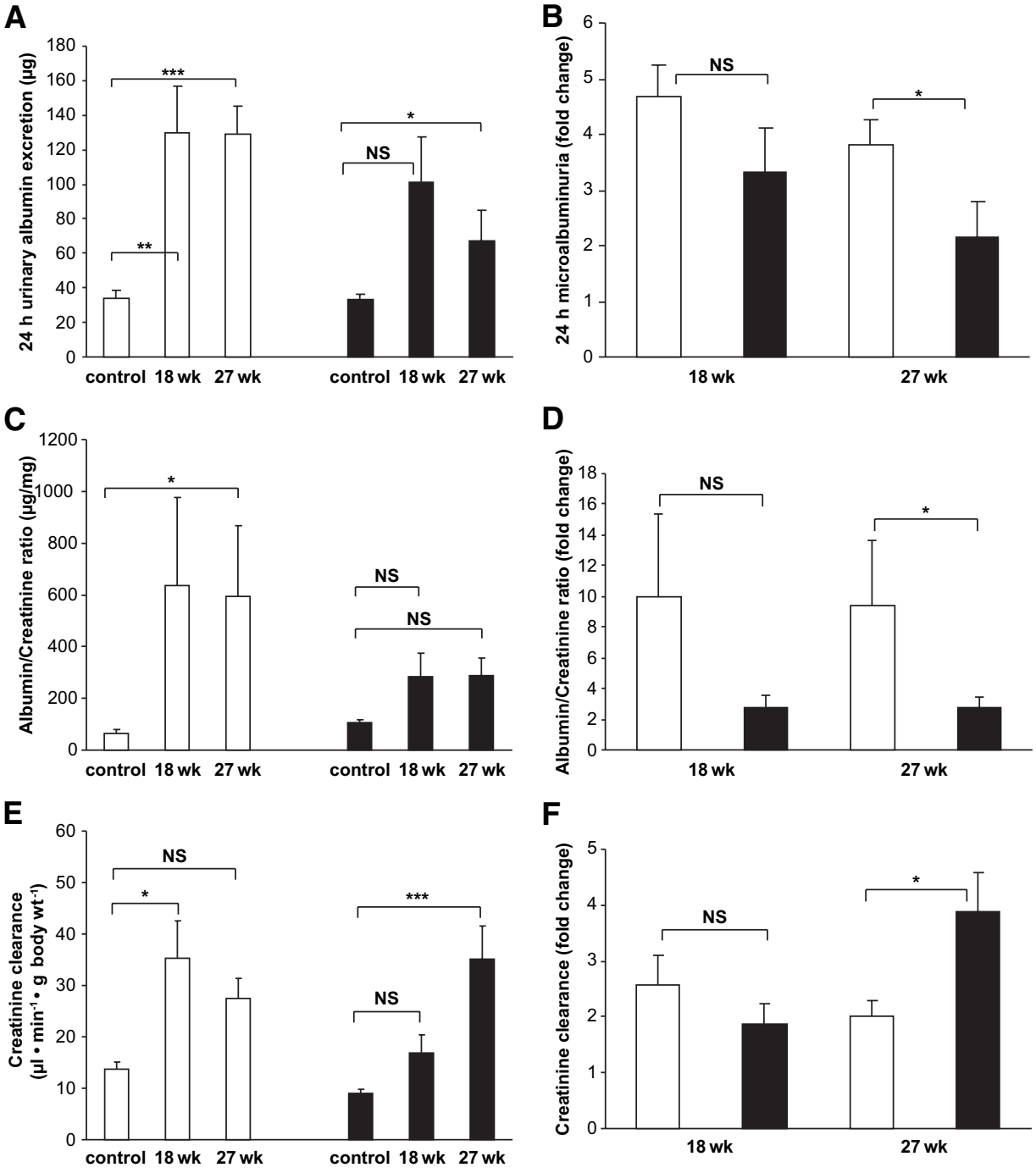

FIG. 5. Renal function impairment is attenuated in diabetic *grem1*$^{+/-}$ mice compared with that in wild-type mice. *A*: Twenty-four–hour urine volumes were measured and levels of microalbumin were measured using an Albuwell M ELISA as described. Values for control nondiabetic (27 weeks), 18-week, and 27-week diabetic groups of wild-type (□) and *grem1*$^{+/-}$ mice (■) were plotted (n = 6–11 per group except *grem1*$^{+/-}$ 18 weeks, n = 3). Data were analyzed using a one-way ANOVA and Tukey-Kramer post hoc analysis. *P < 0.05; **P < 0.01; ***P < 0.001. *B*: Fold change in 24-h microalbuminuria was calculated by divided microalbumin values for individual diabetic wild-type and *grem1*$^{+/-}$ mice by the mean microalbumin value for the corresponding 18- or 27-week control group. Mean fold change values ± SE were plotted. *P < 0.05, using a two-tailed t test. *C*: The ACR was calculated by dividing urinary microalbumin by urinary creatinine and is plotted as micrograms per milliliter. Values from control (nondiabetic), 18-week, and 27-week diabetic wild-type and *grem1*$^{+/-}$ mice were plotted (n = 6–11). *P < 0.05, one-way ANOVA with post hoc Tukey-Kramer multiple comparison test. *D*: Fold change in ACR was calculated by dividing ACR values for individual diabetic wild-type and *grem1*$^{+/-}$ mice by the mean ACR value for the corresponding 18- or 27-week control group. Mean fold change values ± SE were plotted. *P < 0.05, using Student's two-tailed t test. *E*: Creatinine clearance was calculated as microliter per minute per gram body weight. Data from both control and diabetic wild-type and *grem1*$^{+/-}$ mice at time 0, 18 weeks, and 27 weeks of diabetes were plotted (n = 6–11). *P < 0.05; ***P < 0.001, using one-way ANOVA with post hoc Tukey-Kramer multiple comparison test. *F*: Fold change in creatinine clearance was calculated by dividing creatinine clearance values for individual diabetic wild-type and *grem1*$^{+/-}$ mice by the mean creatinine clearance value for the corresponding 18- or 27-week control group. Mean fold change values ± SE were plotted. *P < 0.05 using Student's two-tailed t test. □, wild type; ■, *grem1*$^{+/-}$.

may be linked to a tissue repair mechanism in response to hyperglycemia and other insults that become maladaptive, leading to further kidney injury (23,26). Factors such as TGF-β, AGEs, and hemodynamic stress are features of diabetic nephropathy that have previously been shown to increase *grem1* expression (17,20). Because *grem1*$^{+/-}$

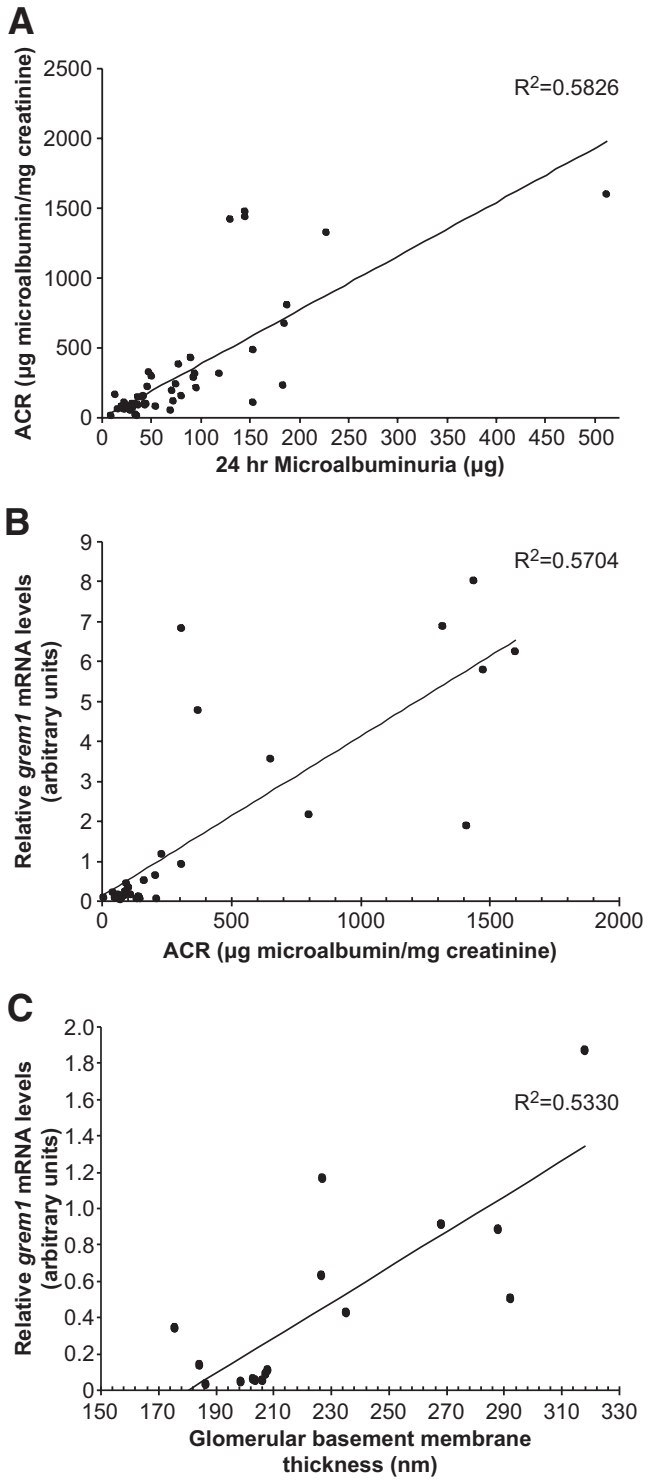

FIG. 6. *grem1* mRNA levels correlate with indexes of renal damage. *A*: Twentyfour microalbumin values (micrograms) were plotted against ACR values (micrograms of microalbumin per milligrams of creatinine) for wild-type and *grem1*$^{+/-}$ control and diabetic mice over the course of the study (n = 50). R^2 value of the trendline was calculated at 0.5846 (n = 49), two-tailed P < 0.0001 using Spearman's rank correlation analysis. *B*: *grem1* mRNA levels were plotted against ACR values for wild-type and *grem1*$^{+/-}$ mice. The cohort of control and diabetic mice of both genotypes at 18 and 27 weeks of diabetes were plotted (n = 30). Spearman rank correlation analysis revealed an R^2 value of 0.5704 with a two-tailed P < 0.0001. (*C*). *grem1* mRNA values were plotted against mean GBM thickness for control and diabetic wild-type and *grem1*$^{+/-}$ mice at 27 weeks of diabetes (n = 17). R^2 = 0.533, two-tailed P < 0.001, using Spearman's rank correlation analysis.

mice displayed a marked reduction in *grem1* upregulation in diabetes (Fig. 2), we propose that the recapitulation of *grem1* gene activation in the diabetic kidney involves both *grem1* alleles.

A similar degree of renal hypertrophy was observed in both wild-type and *grem1*$^{+/-}$ diabetic mice (Table 1). These data suggested that reduction of *grem1* expression prevented diabetes-induced increases in GBM thickness during early-stage diabetic nephropathy. Staining for markers of more advanced kidney damage such as mesangial matrix secretion and interstitial collagen showed modest increases in diabetic mice (Fig. 3*D–F*). Previous data had indicated that C57BL/6J mice were somewhat resistant to diabetic nephropathy–like changes in kidney, manifesting modest increases in albuminuria and glomerular damage (25). Our study also detected modest increases in glomerular damage (Fig. 3), together with a significant increase in microalbuminuria (~4.8-fold) (Fig. 5*A* and *B*). Mice in our study developed severe hyperglycemia (~590 mg/dl) at 18 weeks (Fig. 1*B*). In contrast, C57BL/6 mice in the study of Gurley et al. (25) manifested lower levels of hyperglycemia at 16 weeks (388 mg/dl). Thus, the more robust hyperglycemia in our model may have been sufficient to induce microalbuminuria but not gross structural changes in glomeruli or kidney tubules in our mice. We conclude, based on the early structural changes evident, that our diabetic mice develop mild but significant damage in the kidney and that this early damage is attenuated when levels of *grem1* are reduced by gene deletion. Microalbuminuria developed in wild-type diabetic mice compared with control mice (Fig. 5) but was attenuated in age-matched *grem1*$^{+/-}$ mice (Fig. 5*A* and *B*). Diabetes-induced increases in the ACR were also reduced in *grem1*$^{+/-}$ mice compared with wild-type mice (Fig. 5*C*). Values for creatinine clearance suggest that diabetes-induced hyperfiltration peaked in wild-type mice at 18 weeks (Fig. 5*E*). In contrast, creatinine clearance values for *grem1*$^{+/-}$ diabetic mice were lower at 18 weeks compared with those in wild-type mice and were higher at 27 weeks, suggesting that the peak of hyperfiltration in diabetic *grem1*$^{+/-}$ mice may occur at a later time than that in wild-type mice (Fig. 5*E*). Together with previous data identifying *grem1* upregulation in high-glucose cell culture models and human diabetic nephropathy biopsy specimens, these data add to the growing body of evidence implicating *grem1* in the pathogenesis of diabetic nephropathy. Furthermore, our data provide the first evidence that a reduction in *grem1* expression reduces early impairment of renal structure and function in the diabetic kidney. We are currently examining whether other vascular complications of diabetes are also altered in *grem1*$^{+/-}$ mice. Preliminary evidence from our group suggests that *grem1* deletion may also protect against aortic thickening in the diabetic state, potentially due to altered serum lipid profiles (27).

Several markers of renal damage in diabetes have been identified, and levels of several of these genes were elevated in the wild-type but not *grem1*$^{+/-}$ diabetic kidney (Fig. 7). Thus, in the hyperglycemic state, the triggers that increase the expression of genes contributing to glomerulosclerosis and tubular damage seem to be attenuated in the *grem1*$^{+/-}$ kidney. *grem1* is an antagonist of BMP-2, -4, and -7, binding to these proteins and preventing their interaction with their cognate receptors (6,8,14). Of these, BMP-7 has attracted recent attention, as up to 90% loss of this protein has been reported in the kidneys of diabetic

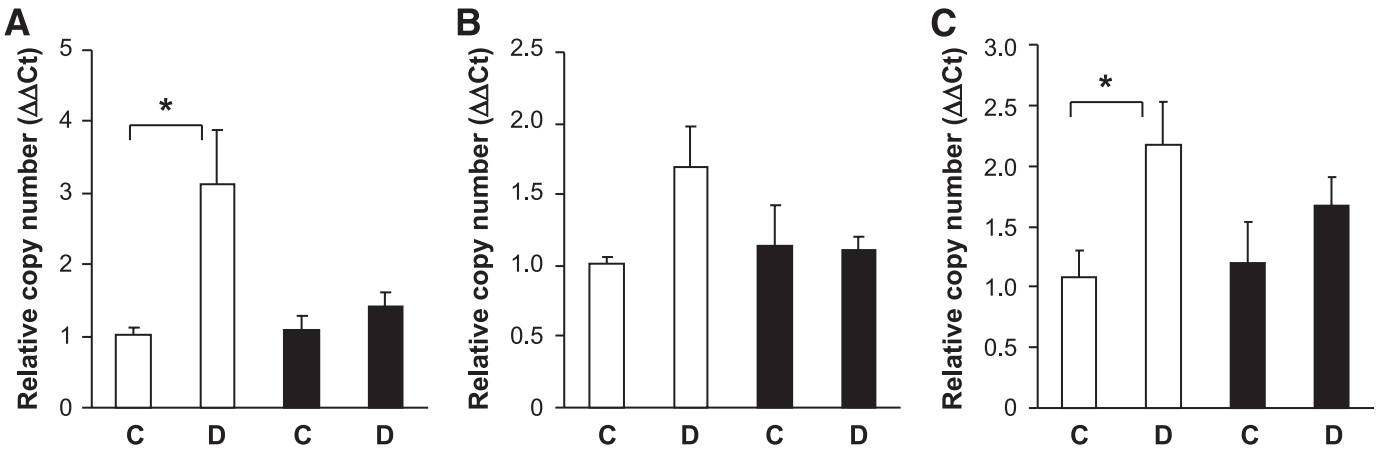

FIG. 7. Upregulation of gene markers of diabetic nephropathy is attenuated in *grem1*$^{+/-}$ mice. Total RNA was extracted from renal poles of control (C) and diabetic (D) wild-type (□) and *grem1*$^{+/-}$ (■) mice at 27 weeks of diabetes. A quantitative TaqMan PCR was performed using mouse fibronectin (*A*), vimentin (*B*), or CTGF (*C*) specific oligonucleotides as described. ΔΔCt values were calculated by subtracting the Ct values for the *18S* control from the corresponding test gene value obtained in the same tube, and altered mRNA levels were then calculated by setting the control in each age-group to 1. Data are plotted as means ± SE. **P* < 0.05, Student's unpaired *t* test, *n* = 4–6 for each group. Increases in vimentin in wild-type diabetic kidney just failed to reach significance (*P* = 0.079).

rats (28). Loss of BMP-7 was accompanied by an increase in *grem1* expression, with both changes probably being driven by increased TGF-β1 in the diabetic kidney (28). Administration of recombinant BMP-7 or transgenic overexpression of BMP-7 in podocytes ameliorates renal injury in mouse models of diabetes (29) and lupus (30). Although significant changes in cellular BMP-7 mRNA or protein were not detected in our diabetic mice (supplementary Fig. 2), our data show that levels of phospho-Smad1/5/8, a downstream target of BMP signaling, were reduced in wild-type but not in *grem1*$^{+/-}$ diabetic kidney compared with control kidneys (Fig. 8), suggesting that loss of *grem1* expression facilitates sustained BMP-7 signaling in the diabetic kidney, extending the notion of a carefully coordinated balance between BMP signaling and *grem1* in the disease state.

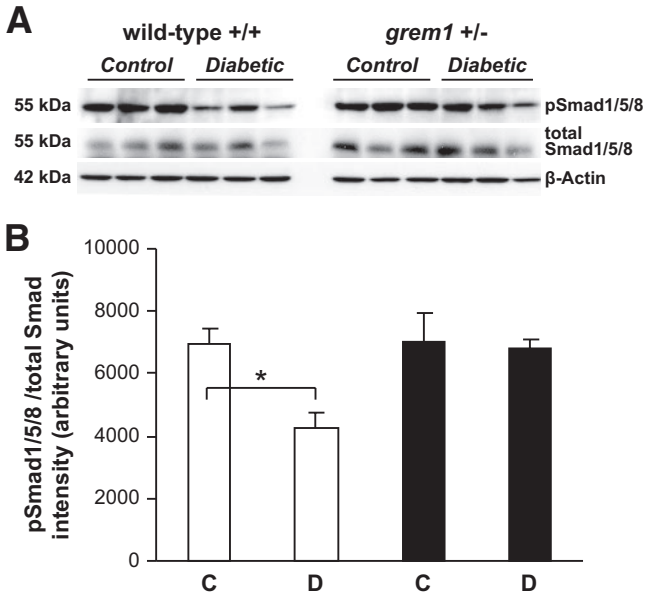

FIG. 8. Decreased pSmad1/5/8 phosphorylation is evident in wild-type but not *grem1*$^{+/-}$ diabetic kidney. *A*: Protein extracts from renal poles of control (C) and 27-week diabetic (D) wild-type (□) and *grem1*$^{+/-}$ (■) mice were probed via Western blot using phospho-Smad1/5/8, total Smad1/5/8, and β-actin antibodies as described. *n* = 3 mice per group. *B*: Densitometry was performed using Scion Image software. pSmad1/5/8 intensities were normalized to total Smad1/5/8 levels and plotted as relative intensity. **P* < 0.05 using Student's unpaired *t* test.

Previous reports have identified other genes such as TGF-β type II receptor, CTGF, and p27^{Kip1} whose deletion confers protection against the sequelae of diabetic kidney disease (31,24,32). p27$^{Kip1+/-}$ mice displayed an intermediate degree of protection compared with that of p27$^{Kip1-/-}$ mice, suggesting that p27^{Kip1} is haploinsufficient in terms of its role in diabetic nephropathy (32). Our data suggest that *grem1* may also be haploinsufficient, as deletion of one allele of *grem1* reduced *grem1* expression and conferred a moderate degree of protection from structural renal damage induced by diabetes.

Because *grem1*$^{+/-}$ mice developed less severe GBM thickening (Fig. 3), together with lower fold increases in ACR and estimated glomerular filtration rate (Fig. 5*C–F*) compared with those in wild-type controls, a reduction in *grem1* levels using gene deletion may reduce both the onset and severity of renal disease in the diabetic kidney. Increased *grem1* levels correlated tightly with both GBM thickening and ACR (Fig. 6), suggesting that reactivation of *grem1* in the diabetic kidney may occur in parallel with early pathological changes in renal structure and function. Because *grem1*$^{+/-}$ mice manifest less severe microalbuminuria and GBM thickening, these data suggest that *grem1* upregulation contributes to glomerular damage in response to diabetes in the kidney.

ACKNOWLEDGMENTS

This work was supported by a Health Research Board of Ireland Clinical Fellowship (CRT/2004/41) to S.A.R. Work in the laboratory of D.P.B. is supported by Science Foundation Ireland and the Health Research Board Ireland. C.G. is supported by Science Foundation Ireland Award 06/IN.1/B114.

No potential conflicts of interest relevant to this article were reported.

We thank Richard Harland for the generous gift of *grem1*$^{+/-}$ knockout mice. Alison Murphy, Laura Connole, George Keating, Joe Mooney, Alfie Redmond (University College Dublin), and Brendan Tobin (Mater Hospital) are gratefully acknowledged for excellent technical assistance. We thank Dionne van der Giezen (Utrecht) for

histology analysis and quantitation. We acknowledge Jay Jerome and the excellent collaboration with the Vanderbilt University Medical Center (VUMC) Research Electron Microscopy Core (sponsored by National Institutes of Health Grants DK20539, CA68485, and DK58404) as well as the VUMC Mouse Metabolic Phenotyping Core (Grant DK59637).

Parts of this study were presented as a poster at the annual meeting of the American Society of Nephrology, San Francisco, California, 31 October–5 November 2007.

REFERENCES

1. Ritz E, Rychlik I, Locatelli F, Halimi S. End-stage renal failure in type 2 diabetes: a medical catastrophe of worldwide dimensions. Am J Kidney Dis 1999;34:795–808
2. Tan AL, Forbes JM, Cooper ME. AGE, RAGE, and ROS in diabetic nephropathy. Semin Nephrol 2007;27:130–143
3. Isono M, Chen S, Hong SW, Iglesias-de la Cruz MC, Ziyadeh FN. Smad pathway is activated in the diabetic mouse kidney and Smad3 mediates TGF-beta-induced fibronectin in mesangial cells. Biochem Biophys Res Commun 2002;296:1356–1365
4. Kattla JJ, Carew RM, Heljic M, Godson C, Brazil DP. Protein kinase B/Akt activity is involved in renal TGF-β1-driven epithelial-mesenchymal transition in vitro and in vivo. Am J Physiol Renal Physiol 2008;295:F215–F225
5. Sakai N, Wada T, Furuichi K, Iwata Y, Yoshimoto K, Kitagawa K, Kokubo S, Kobayashi M, Hara A, Yamahana J, Okumura T, Takasawa K, Takeda S, Yoshimura M, Kida H, Yokoyama H. Involvement of extracellular signal-regulated kinase and p38 in human diabetic nephropathy. Am J Kidney Dis 2005;45:54–65
6. Hsu DR, Economides AN, Wang X, Eimon PM, Harland RM. The *Xenopus* dorsalizing factor Gremlin identifies a novel family of secreted proteins that antagonize BMP activities. Mol Cell 1998;1:673–683
7. Topol LZ, Bardot B, Zhang Q, Resau J, Huillard E, Marx M, Calothy G, Blair DG. Biosynthesis, post-translation modification, and functional characterization of Drm/Gremlin. J Biol Chem 2000;275:8785–8793
8. Merino R, Rodriguez-Leon J, Macias D, Ganan Y, Economides AN, Hurle JM. The BMP antagonist Gremlin regulates outgrowth, chondrogenesis and programmed cell death in the developing limb. Development 1999;126:5515–5522
9. Michos O, Goncalves A, Lopez-Rios J, Tiecke E, Naillat F, Beier K, Galli A, Vainio S, Zeller R. Reduction of BMP4 activity by gremlin 1 enables ureteric bud outgrowth and GDNF/WNT11 feedback signalling during kidney branching morphogenesis. Development 2007;134:2397–2405
10. Khokha MK, Hsu D, Brunet LJ, Dionne MS, Harland RM. Gremlin is the BMP antagonist required for maintenance of Shh and Fgf signals during limb patterning. Nat Genet 2003;34:303–307
11. Michos O, Panman L, Vintersten K, Beier K, Zeller R, Zuniga A. Gremlin-mediated BMP antagonism induces the epithelial-mesenchymal feedback signaling controlling metanephric kidney and limb organogenesis. Development 2004;131:3401–3410
12. Gazzerro E, Smerdel-Ramoya A, Zanotti S, Stadmeyer L, Durant D, Economides AN, Canalis E. Conditional deletion of gremlin causes a transient increase in bone formation and bone mass. J Biol Chem 2007;282:31549–31557
13. Gazzerro E, Pereira RC, Jorgetti V, Olson S, Economides AN, Canalis E. Skeletal overexpression of gremlin impairs bone formation and causes osteopenia. Endocrinology 2005;146:655–665
14. Costello CM, Howell K, Cahill E, McBryan J, Konigshoff M, Eickelberg O, Gaine S, Martin F, McLoughlin P. Lung-selective gene responses to alveolar hypoxia: potential role for the bone morphogenetic antagonist gremlin in pulmonary hypertension. Am J Physiol Lung Cell Mol Physiol 2008;295:L272–L284
15. Stabile H, Mitola S, Moroni E, Belleri M, Nicoli S, Coltrini D, Peri F, Pessi A, Orsatti L, Talamo F, Castronovo V, Waltregny D, Cotelli F, Ribatti D, Presta M. Bone morphogenic protein antagonist Drm/gremlin is a novel proangiogenic factor. Blood 2007;109:1834–1840
16. Murphy M, Godson C, Cannon S, Kato S, Mackenzie HS, Martin F, Brady HR. Suppression subtractive hybridization identifies high glucose levels as a stimulus for expression of connective tissue growth factor and other genes in human mesangial cells. J Biol Chem 1999;274:5830–5834
17. McMahon R, Murphy M, Clarkson M, Taal M, Mackenzie HS, Godson C, Martin F, Brady HR. IHG-2, a mesangial cell gene induced by high glucose, is human gremlin: regulation by extracellular glucose concentration, cyclic mechanical strain, and transforming growth factor-beta1. J Biol Chem 2000;275:9901–9904
18. Dolan V, Murphy M, Alarcon P, Brady HR, Hensey C. Gremlin—a putative pathogenic player in progressive renal disease. Expert Opin Ther Targets 2003;7:523–526
19. Dolan V, Murphy M, Sadlier D, Lappin D, Doran P, Godson C, Martin F, O'Meara Y, Schmid H, Henger A, Kretzler M, Droguett A, Mezzano S, Brady HR. Expression of gremlin, a bone morphogenetic protein antagonist, in human diabetic nephropathy. Am J Kidney Dis 2005;45:1034–1039
20. Walsh DW, Roxburgh SA, McGettigan P, Berthier CC, Higgins DG, Kretzler M, Cohen CD, Mezzano S, Brazil DP, Martin F. Co-regulation of Gremlin and Notch signalling in diabetic nephropathy. Biochim Biophys Acta 2008;1782:10–21
21. Mezzano S, Droguett A, Burgos ME, Aros C, Ardiles L, Flores C, Carpio D, Carvajal G, Ruiz-Ortega M, Egido J. Expression of gremlin, a bone morphogenetic protein antagonist, in glomerular crescents of pauci-immune glomerulonephritis. Nephrol Dial Transplant 2007;22:1882–1890
22. Carvajal G, Droguett A, Burgos ME, Aros C, Ardiles L, Flores C, Carpio D, Ruiz-Ortega M, Egido J, Mezzano S. Gremlin: a novel mediator of epithelial mesenchymal transition and fibrosis in chronic allograft nephropathy. Transplant Proc 2008;40:734–739
23. Roxburgh SA, Murphy M, Pollock CA, Brazil DP. Recapitulation of embryological programmes in renal fibrosis—the importance of epithelial cell plasticity and developmental genes. Nephron Physiol 2006;103:139–148
24. Nguyen TQ, Roestenberg P, van Nieuwenhoven FA, Bovenschen N, Li Z, Xu L, Oliver N, Aten J, Joles JA, Vial C, Brandan E, Lyons KM, Goldschmeding R. CTGF Inhibits BMP-7 Signaling in diabetic nephropathy. J Am Soc Nephrol 2008;19:2098–2107
25. Gurley SB, Clare SE, Snow KP, Hu A, Meyer TW, Coffman TM. Impact of genetic background on nephropathy in diabetic mice. Am J Physiol Renal Physiol 2006;290:F214–F222
26. Lappin DW, McMahon R, Murphy M, Brady HR. Gremlin: an example of the re-emergence of developmental programmes in diabetic nephropathy. Nephrol Dial Transplant 2002;17 (Suppl. 9):65–67
27. Curran SP, Watson AJ, Brazil DP: The effect of alleic deletion of Gremlin on vascular complications associated with a mouse model of type 1 diabetic nephropathy. J Am Soc Nephrol 2008;19:411A
28. Wang SN, Lapage J, Hirschberg R. Loss of tubular bone morphogenetic protein-7 in diabetic nephropathy. J Am Soc Nephrol 2001;12:2392–2399
29. Wang S, de Caestecker M, Kopp J, Mitu G, Lapage J, Hirschberg R. Renal bone morphogenetic protein-7 protects against diabetic nephropathy. J Am Soc Nephrol 2006;17:2504–2512
30. Zeisberg M, Bottiglio C, Kumar N, Maeshima Y, Strutz F, Muller GA, Kalluri R. Bone morphogenic protein-7 inhibits progression of chronic renal fibrosis associated with two genetic mouse models. Am J Physiol Renal Physiol 2003;285:F1060–1067
31. Kim HW, Kim BC, Song CY, Kim JH, Hong HK, Lee HS. Heterozygous mice for TGF-βIIR gene are resistant to the progression of streptozotocin-induced diabetic nephropathy. Kidney Int 2004;66:1859–1865
32. Wolf G, Schanze A, Stahl RA, Shankland SJ, Amann K. p27^{Kip1} Knockout mice are protected from diabetic nephropathy: evidence for p27^{Kip1} haplotype insufficiency. Kidney Int 2005;68:1583–1589